

1 **Impacts of Varying Model Physics on Simulated Structures in a Cold Air**

2 **Outbreak Cloud System**

3 Andrew T. Lesage\* and Steven K. Krueger

4 *Department of Atmospheric Sciences, University of Utah, Salt Lake City, Utah*

5 \*Corresponding author address: Andrew T. Lesage, Department of Atmospheric Sciences, 135 S

6 1460 E, Rm 819, Salt Lake City, Utah 84112-0110.

7 E-mail: andy.lesage@utah.edu

## ABSTRACT

- 8 Put in an abstract.

## 9 **1. Introduction**

10 Turbulence parameterization methodology has had an important role in model handling of  
11 clouds. Early versions of turbulence parameterizations used a diagnostic equation to solve for  
12  $K$ , the eddy viscosity (Pielke 1974). Other methods sought a prognostic turbulent kinetic energy  
13 (TKE) equation though even second-moment schemes at times had difficulty with vertical trans-  
14 port of TKE (Yamada and Mellor 1975). Third-moment turbulent closure schemes have been used  
15 to better capture TKE in the boundary layer and in-cloud (Krueger 1988).

## 16 **2. Model Background**

## 17 **3. CONSTRAIN Model Setup**

18 The grey zone is the range of grid sizes in atmospheric model simulations that are between  
19 high resolution scales which can adequately resolve turbulence ( $< 1$  km) to low resolution scales  
20 which require convective parameterization ( $> 10$  km). This range is critical in handling modeling  
21 questions from topics as diverse as the Madden-Julian Oscillation (MJO) (Wang et al. 2015),  
22 tropical cyclones (Sun et al. 2014), stratocumulus (Boutle et al. 2014), and the convective boundary  
23 layer (Shin and Hong 2015).

24 The Grey Zone Project was designed to explore model behavior with and without convective  
25 parameterization at grid sizes throughout the grey zone in order to better understand model per-  
26 formance. A case study selected for intercomparison is from CONSTRAIN, a Met Office field  
27 campaign in January 2010 over the North Atlantic ocean. The specific day selected is a cold-air  
28 outbreak event on 31 January 2010. Cold-air outbreak cases have been shown to have convec-  
29 tion morph from organized rolls to open cellular convection, which can have significant impacts  
30 on transport of heat and moisture (Brümmer 1999; Brümmer and Pohlmann 2000). The case is

31 14.5 hours in duration with initial conditions and forcings generated from high resolution limited  
32 area model simulations performed by Paul Field on the Met Office Unified Model (UM) (Field  
33 et al. 2014). Model simulations for this event have been compared to aircraft, satellite, and radar  
34 observations (Field et al. 2014; McBeath et al. 2014).

35 For the CONSTRAIN case, SAM runs without SHOC at .1 km were used as the LES baseline  
36 run for each set of model physics. From there, many other runs were performed, outlined in Table  
37 1. Sets of runs at varying grid resolution for NOSHOCS were run for full physics, no radiation, and  
38 no ice configurations. Sets of runs for SHOC were performed for full physics, no radiation, no ice,  
39 ice only, no ice sedimentation, and no ice/sedimentation/precipitation configurations. Additional  
40 runs were performed for no precipitation, and no radiation/precipitation configurations. Peter  
41 Bogenschutz also ran LES and 3 km SHOC and NOSHOCS simulations using the Morrison M2005  
42 double-moment microphysics scheme.

#### 43 **4. Results**

44 Model profiles were made by averaging the last hour of model output. The profiles for total  
45 cloud water are shown in Figure 1. For most of the runs, the NOSHOCS and SHOC runs are fairly  
46 representative of the LES runs with slight differences in maximum total cloud water elevation and  
47 total cloud water amount. For no sedimentation runs, the maximum total cloud water amount is  
48 underestimated in the SHOC runs. The lower resolution no ice runs (8 km for SHOC, 3 km for  
49 NOSHOCS) have slightly larger differences from the LES baseline than the higher resolution no ice  
50 runs. Since most of the TKE is resolved at grid sizes up to 3 km, the differences between SHOC  
51 and NOSHOCS remain small.

52 Time series for LES runs of surface precipitation rate, cloud water path (CWP) + ice water  
53 path (IWP), and cloud shield fraction are shown in Figure 2. Precipitation rates are higher in

54 the full physics run than the no radiation run; however, the difference in CWP + IWP and cloud  
55 shield fraction is very small in the precipitation allowing runs for full physics vs no radiation.  
56 Cloud fraction is larger in no precipitation runs and much larger for the full physics run without  
57 precipitation than the no radiation run without precipitation.

58 Effects of cloud ice and ice sedimentation for LES runs are shown in Figure 3. The full physics  
59 run has a higher cloud fraction than the ice only run at a higher level, just over 1 km for full physics  
60 compared to just over 0.5 km for ice only. The runs without ice sedimentation had much higher  
61 cloud fractions with a maximum at roughly 2.25 km. Total TKE was higher throughout the entire  
62 profile for the no ice sedimentation runs which shows these runs have higher entrainment than the  
63 runs that allow for ice sedimentation.

64 The effects of the microphysics scheme selection along with additional no ice and no ice sed-  
65 imentation choices on LES runs is shown in Figure 4. Surface precipitation rate increases faster  
66 in the full physics and no ice sedimentation runs; however, the double-moment (M2005) micro-  
67 physics run has the highest surface precipitation rate of the four at around 14 hours. The no ice  
68 run is the slowest to develop precipitation. CWP + IWP stays lower for the runs with higher pre-  
69 cipitation and highest for the no ice run. The microphysics scheme makes a significant difference  
70 in IWP as the M2005 run only develops a minute fraction of IWP relative to the single-moment  
71 full physics run. Inversion height generally trends upward over time though is much slower for the  
72 full physics run which decreases slightly in inversion height the first five hours.

## 73 **5. Conclusions**

74 Add in conclusions.

75 *Acknowledgments.* CONSTRAIN runs using the M2005 microphysics were run by Peter Bo-  
76 genschutz. This research was supported by the Office of Science (BER), U. S. Department of

77 Energy, and by the National Science Foundation Science and Technology Center for Multi-Scale  
78 Modeling of Atmospheric Processes, managed by Colorado State University under cooperative  
79 agreement No. ATM-0425247.

## 80 **References**

81 Boutle, I. A., J. E. J. Eyre, and A. P. Lock, 2014: Seamless stratocumulus simulation across the  
82 turbulent gray zone. *Mon. Wea. Rev.*, **142**, 1655–1668., doi:10.1175/MWR-D-13-00229.1.

83 Brümmer, B., 1999: Roll and cell convection in wintertime Arctic cold-air outbreaks. *J. Atmos.*  
84 *Sci.*, **56**, 2613–2636, doi:10.1175/1520-0469(1999)056<2613:RACCIW>2.0.CO;2.

85 Brümmer, B., and S. Pohlmann, 2000: Wintertime roll and cell convection over Greenland and  
86 Barents Sea regions: A climatology. *J. Geophys. Res.*, **105(D12)**, 15 559–15 566, doi:10.1029/  
87 1999JD900841.

88 Field, P. R., R. J. Cotton, K. McBeath, A. P. Lock, S. Webster, and R. P. Allan, 2014: Improving  
89 a convection-permitting model simulation of a cold air outbreak. *J. Atmos. Sci.*, **140**, 124–138.,  
90 doi:10.1002/qj.2116.

91 Krueger, S. K., 1988: Numerical simulation of tropical cumulus clouds and their interaction with  
92 the subcloud layer. *J. Atmos. Sci.*, **45**, 2221–2250., doi:10.1175/1520-0469(1988)045<2221:  
93 NSOTCC>2.0.CO;2.

94 McBeath, K., P. R. Field, and R. J. Cotton, 2014: Using operational weather radar to assess high-  
95 resolution numerical weather prediction over the British Isles for a cold air outbreak case-study.  
96 *Q. J. R. Meteorol. Soc.*, **140**, 225–239., doi:10.1002/qj.2123.

97 Pielke, R. A., 1974: A three-dimensional numerical model of the sea breezes over South Florida.  
98 *Mon. Wea. Rev.*, **102**, 115–139., doi:10.1175/1520-0493(1974)102<0115:ATDNMO>2.0.CO;2.

- 99 Shin, H. H., and S.-Y. Hong, 2015: Representation of the subgrid-scale turbulent transport in  
100 convective boundary layers at gray-zone resolutions. *Mon. Wea. Rev.*, **143**, 250–271., doi:10.  
101 1175/MWR-D-14-00116.1.
- 102 Sun, Y., L. Yi, Z. Zhong, and Y. Ha, 2014: Performance of a new convective parameterization  
103 scheme on model convergence in simulations of a tropical cyclone at grey-zone resolutions. *J.*  
104 *Atmos. Sci.*, **71**, 2078–2088., doi:10.1175/JAS-D-13-0285.1.
- 105 Wang, S., A. H. Sobel, F. Zhang, Y. Q. Sun, Y. Yue, and L. Zhou, 2015: Regional simulation of  
106 the October and November MJO events during the CINDY/DYNAMO field campaign at gray  
107 zone resolution. *J. Climate.*, **28**, 2097–2119., doi:10.1175/JCLI-D-14-00294.1.
- 108 Yamada, T., and G. Mellor, 1975: A simulation of the Wangara atmospheric boundary layer data.  
109 *J. Atmos. Sci.*, **32**, 2309–2329., doi:10.1175/1520-0469(1975)032<2309:ASOTWA>2.0.CO;2.

110 **LIST OF TABLES**

111 **Table 1.** Model simulations performed for the CONSTRAIN case study. . . . . 9

TABLE 1. Model simulations performed for the CONSTRAIN case study.

	SHOC						NOSHOC				
Grid Spacing	30 km	8 km	4 km	3 km	1 km	.5 km	30 km	3 km	1 km	.5 km	.1 km
Full Physics	x			x	x	x	x	x	x	x	x
No Precipitation					x	x					x
No Rad.	x			x	x	x	x	x	x	x	x
No Rad./Prec.											x
No Ice	x	x		x	x	x		x	x	x	x
Ice Only	x			x	x	x					x
No Sed.				x	x	x					x
No Ice/Sed./Prec.		x	x		x						x
M2005				x				x			x

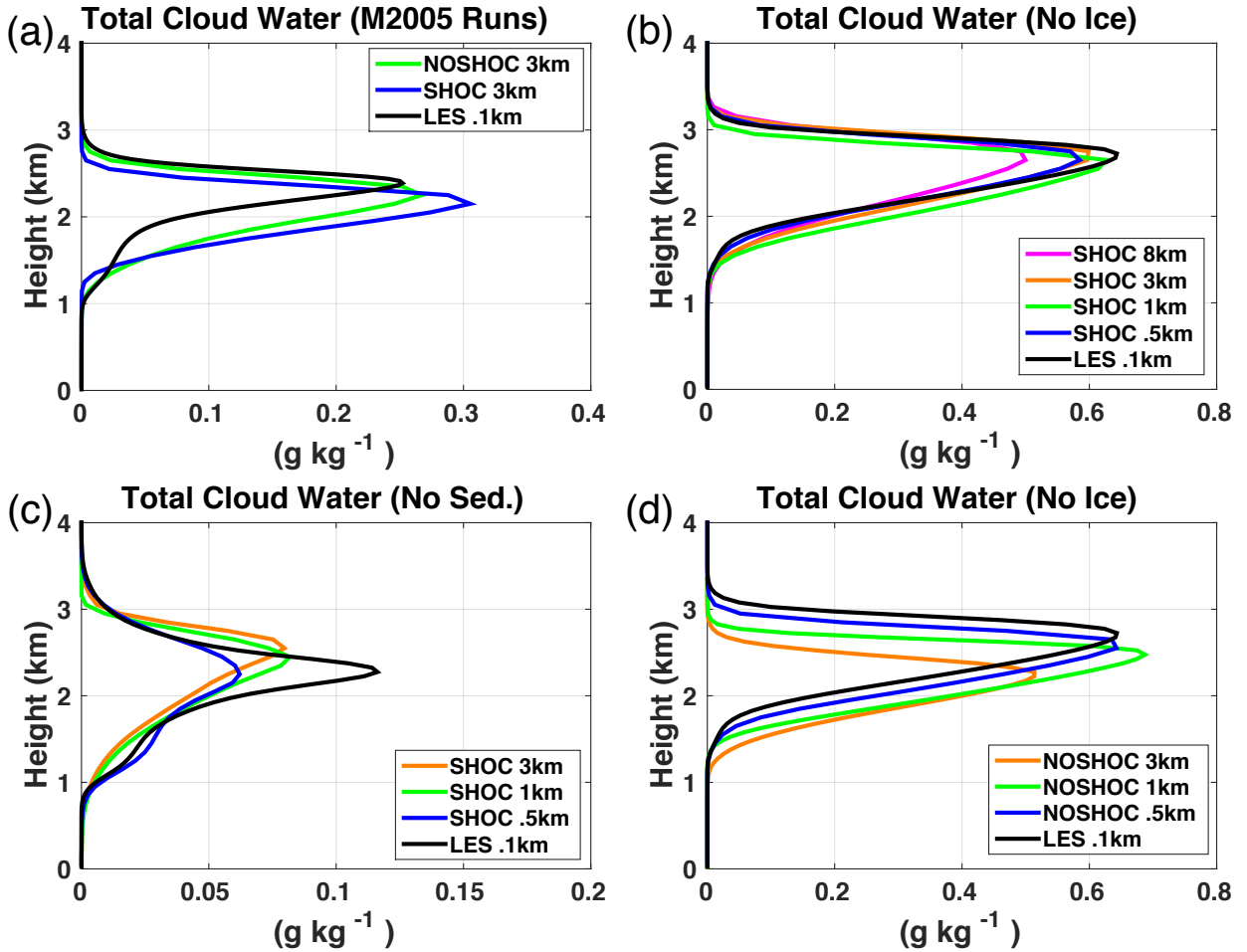
112 **LIST OF FIGURES**

113 **Fig. 1.** Final-hour averaged total cloud water profiles of CONSTRAIN simulations for: a) double-  
114 moment microphysics runs, b) no ice runs with SHOC, c) no ice sedimentation runs, and  
115 d) no ice runs without SHOC. LES runs in each plot panel are high resolution runs used as  
116 benchmarks. Note: x-axis scales are different among the panels. . . . . 11

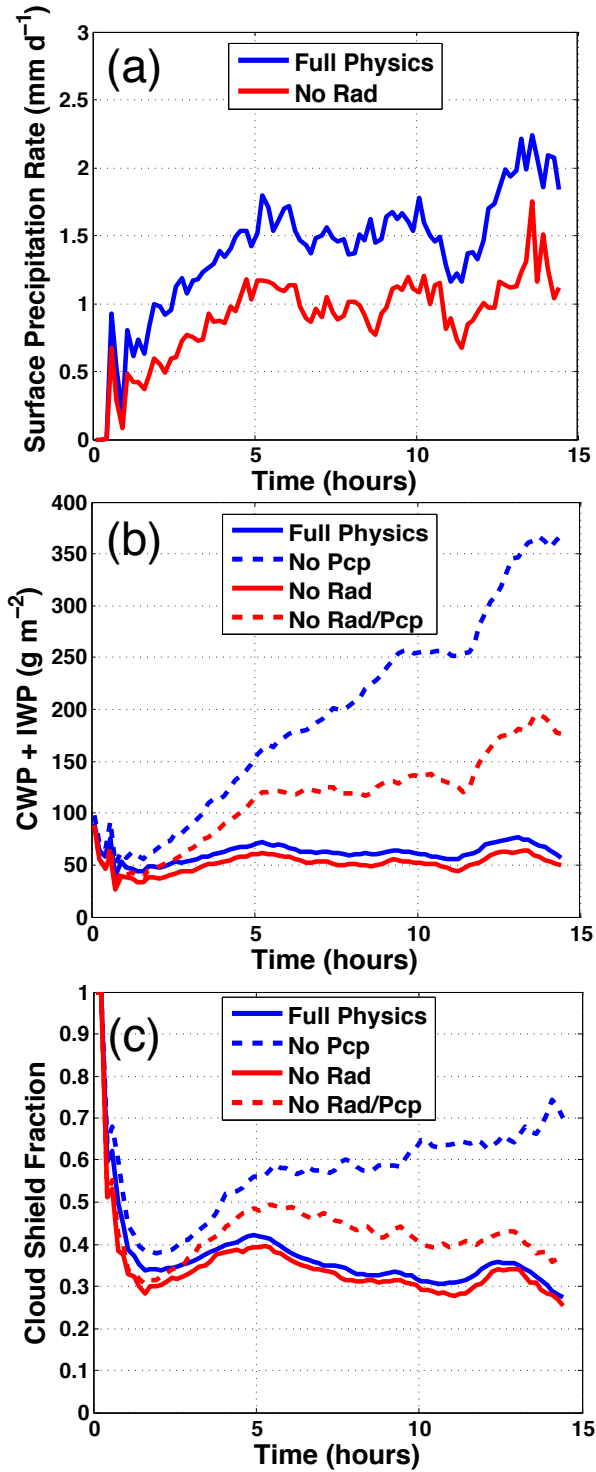
117 **Fig. 2.** CONSTRAIN LES time series of full physics, no precipitation, no radiation, and no radi-  
118 ation or precipitation runs for a) surface precipitation rate, b) cloud water path + ice water  
119 path, and c) cloud shield fraction. . . . . 12

120 **Fig. 3.** Final-hour averaged CONSTRAIN LES profiles of a) cloud fraction, b) total cloud water  
121 and ice, and c) total turbulent kinetic energy for full physics, no ice sedimentation, ice only,  
122 and ice only + no ice sedimentation runs. . . . . 13

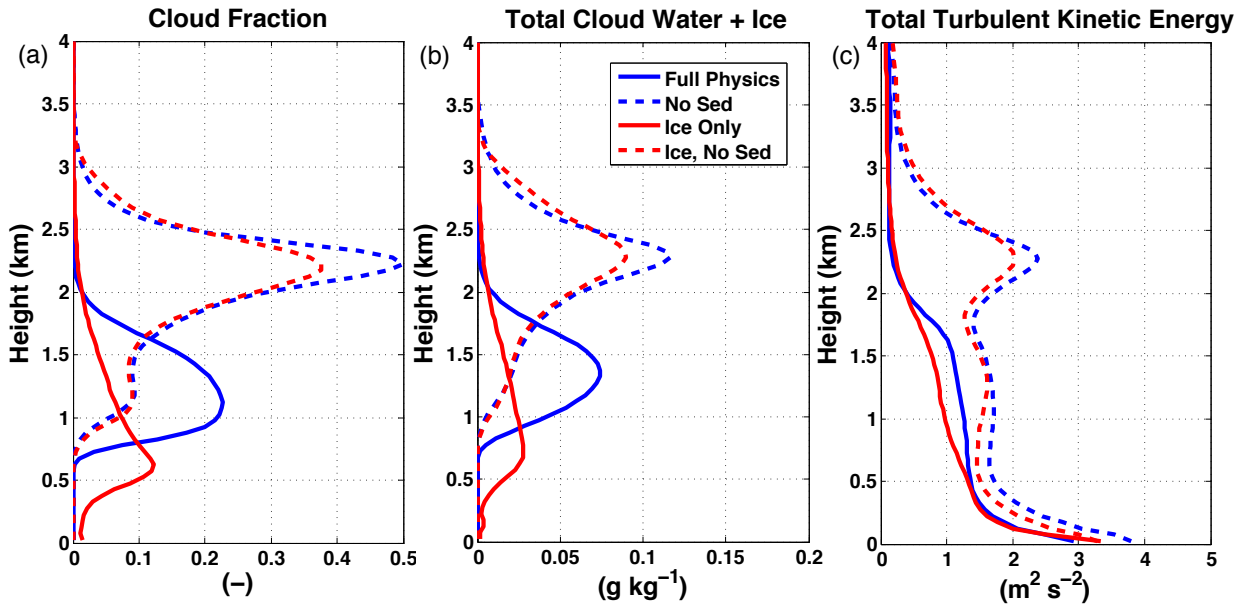
123 **Fig. 4.** CONSTRAIN LES time series of full physics, Morrison (2005) double-moment micro-  
124 physics, no ice sedimentation, and no ice runs for a) surface precipitation rate, b) cloud  
125 water path + ice water path, c) ice water path, and d) inversion height. . . . . 14



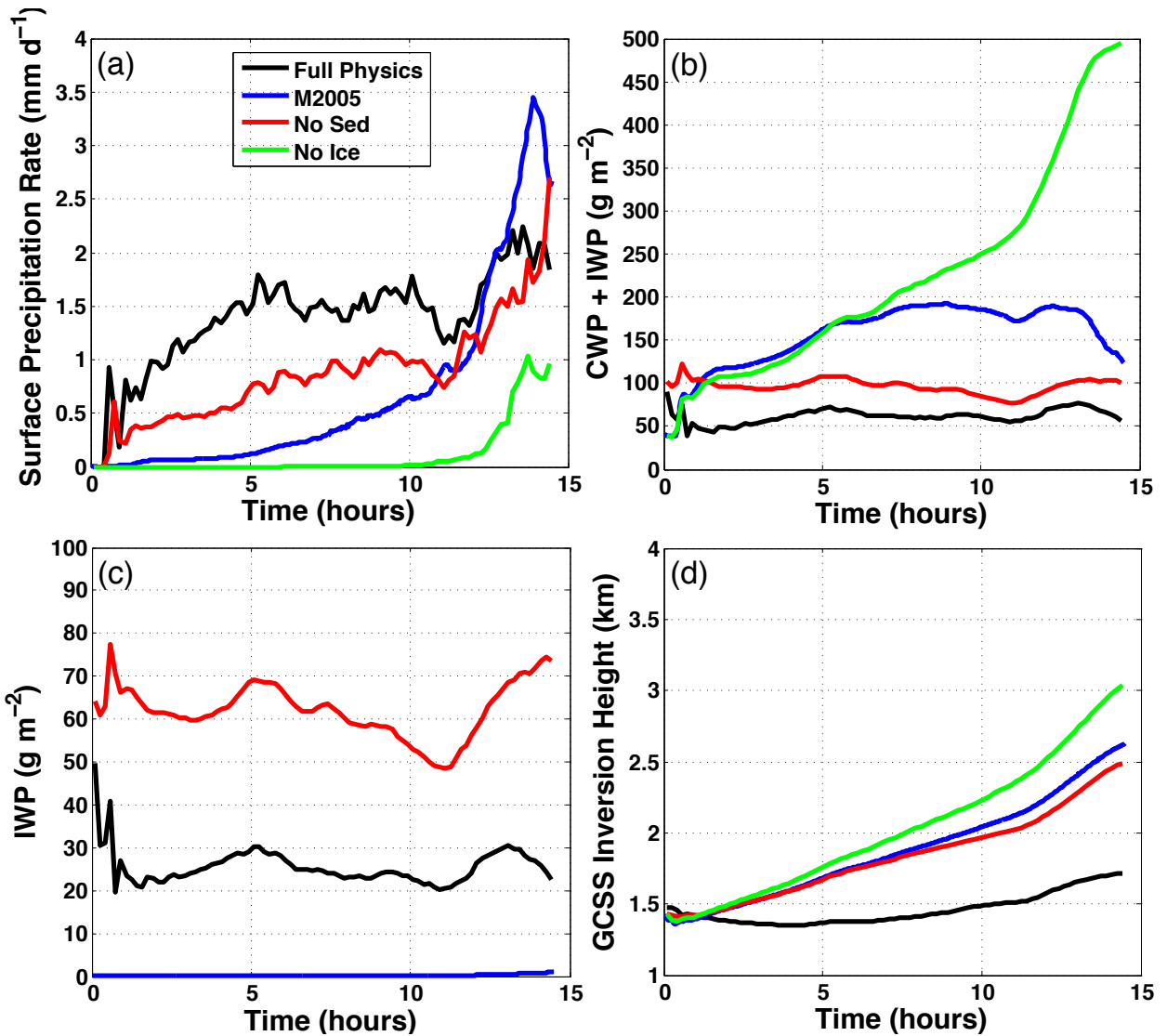
126 FIG. 1. Final-hour averaged total cloud water profiles of CONSTRRAIN simulations for: a) double-moment  
 127 microphysics runs, b) no ice runs with SHOC, c) no ice sedimentation runs, and d) no ice runs without SHOC.  
 128 LES runs in each plot panel are high resolution runs used as benchmarks. Note: x-axis scales are different  
 129 among the panels.



130 FIG. 2. CONSTRAN LES time series of full physics, no precipitation, no radiation, and no radiation or  
 131 precipitation runs for a) surface precipitation rate, b) cloud water path + ice water path, and c) cloud shield  
 132 fraction.



133 FIG. 3. Final-hour averaged CONSTRAN LES profiles of a) cloud fraction, b) total cloud water and ice,  
 134 and c) total turbulent kinetic energy for full physics, no ice sedimentation, ice only, and ice only + no ice  
 135 sedimentation runs.



136 FIG. 4. CONSTRAIN LES time series of full physics, Morrison (2005) double-moment microphysics, no ice  
 137 sedimentation, and no ice runs for a) surface precipitation rate, b) cloud water path + ice water path, c) ice water  
 138 path, and d) inversion height.